A New Multi-Link Time-Reversal Prefilter Design for Indoor Wireless Communications

MISUN YOON[1], DUCKDONG HWANG[2], (Member, IEEE), AND CHUNGYONG LEE[3], (Member, IEEE)

[1]Network Business, Samsung Electronics Company Ltd., Suwon 16677, South Korea
[2]Department of Information and Communication Engineering, Sejong University, Seoul 05006, South Korea
[3]School of Electrical and Electronic Engineering, Yonsei University, Seoul 03722, South Korea

Corresponding author: Chungyong Lee (cylee@yonsei.ac.kr)

ABSTRACT A prefilter based on the time-reversal (TR) is proposed to control the multi-link interference (MLI) and the inter-symbol interference (ISI) for multi-link system. At first, we define a new parameter signal-to-sidelobe-plus-leakage ratio (SSLR) to represent the performance of the multi-link system. To improve the bit error rate (BER) performance, the proposed prefilter minimizes the MLI and the ISI and maximizes the peak power of received signal at the same time by maximization of the SSLR. We set an optimization problem to maximize the SSLR which is a quadratically constrained fractional quadratic problem. To solve the optimization problem, we use the epigraph form and the bisection method. Therefore, we find an ε-optimal solution which is a global optimal solution. Simulation results show that link interference power is reduced by the MLI-TR prefilter and the SSLR of the MLI-TR prefilter is higher than that of the conventional TR prefilter. Moreover, the BER performance of the MLI-TR prefilter is improved in overall signal-to-noise ratio range.

INDEX TERMS Time-reversal prefilter, indoor radio communication, interference channels, signal processing, optimization.

I. INTRODUCTION

Recently, ultra wideband (UWB) communication system has received attention since it is appropriate for high-speed communication in short distance [1]. Thanks to the large bandwidth, the UWB communication system can support high data rate transmission. However, there are dense multipaths and long delay spread which cause performance degradation [2]. To resolve individual multipath component, many researches have been performed for short range communication techniques such as rake receiver and energy detector. The rake receiver uses many fingers to gather sufficient energy enough for the target signal-to-noise ratio (SNR) [3]. However, it is too complex to be implemented in the receiver for the short range communication which should have very small and simple structure. To reduce the complexity of the receiver, many non-coherent schemes were studied in [4]–[9]. However, the performances of these receivers are still degraded significantly because they cannot mitigate the interference in multipath channel. More-

over, in multi-user systems, especially in multi-link systems where there are multiple transceivers in [10] and [11], the receiver performances are severely affected by multi-link interference.

To combat the performance degradation from the delay spread, the time-reversal (TR) prefilter was proposed [12]. The TR prefilter has been studied in the ultrasound medical imaging and the underwater communications [13]. Recently, it has attracted attention due to simple structure for indoor wireless communication [14]–[21]. Since the TR prefilter shifts the design complexity from receiver to transmitter, the receiver uses a single-tap detector. The TR prefilter uses the time-reversed channel impulse response (CIR) as a prefilter. The receiver sends an impulse to the transmitter, and then the transmitter estimates the CIR and exploits the channel reciprocity for prefilter design [12]. The transmitted signal from the TR prefilter retraces the channel. Thus, the energy of the received signal is concentrated within few taps and the sidelobes are reduced - temporal focusing effect [16]. Moreover, the transmitted signal is focused at the intended receiver - spatial focusing effect [16]. Through the TR prefilter, the inter-symbol interference (ISI) and the

---

The associate editor coordinating the review of this manuscript and approving it for publication was Ebrahim Bedeer.

multi-link interference (MLI) are reduced without complexity increase.

Based on the advantages of the TR prefilter, there are many researches to apply the TR prefilter to the indoor wireless communication. The space-time reversal prefilters was proposed in [18] and the TR prefilter with the MMSE receiver was studied in [19] to reduce the ISI. Reference [20] proposed an improved TR prfilter for a single link system to maximize signal-to-sidelobe ratio (SSR). In [21], equalized TR (ETR), which uses equalizer cascaded with the TR prefilters for minimizing the ISI power at the receiver, was proposed and theoretical performance bounds for ETR was also derived. Some of researches about the multi-user system have been carried out. In [22], the modified TR prefilter using circular shift operation was proposed. The time reversal division multiple access (TRDMA) scheme was proposed in [23] and [24] to support multi-users. This concept has been extended in [25] to apply in massive MIMO systems. Moreover, the authors in [26] and [27] apply the TR prefilter to the millimeter-wave MIMO system with interference nulling and hybrid beamforming schemes. In [28], the SNR of target receiver and unintended receiver with distributed time reversal (DTR) scheme is analyzed. However, only few researches have been considered the multi-link system recently. The authors in [29] proposed the application of TR prefilter to heterogeneous network in limited backhaul connection. In [30], the physical-layer security issue in multiple-input single-output (MISO) UWB systems was addressed for various types of TR prefilters which exploit the spatial domain for increasing the received power for legitimate user while suppressing the received power for the eavesdropper. In [31], the authors provided an overview for the adequacy of the TR for the system with a number of devices such as internet-of-things (IoT) systems. In [32], the authors considered the TR technique in multi-cell UWB systems. It provided the feasibility of the MLI on the TR prefilter, though the consideration on the multi-link interference mitigation is limited. The authors in [33] also proposed a waveform design for downlink multi-user systems. Though [33] considered the inter-user interference, it is not easy to be extended to multi-link systems. In this paper, we consider a TR prefilter for the multi-link indoor wireless communication system. As the number of links increases, the MLI is a principal factor for performance degradation. Thus, it is important to control the MLI and the ISI in the indoor wireless communication. We propose a novel prefilter based on the TR prefilter to mitigate the ISI and the MLI. The proposed prefilter maintains the peak power of the received signal to be robust to noise. In order to mitigate the ISI and the MLI and maximize the peak power of the received signal at the same time, we define a new parameter signal-to-sidelobe-plus-leakage ratio (SSLR). We establish an optimization problem for the proposed prefilter to maximize the SSLR.

The optimization problem is a quadratically constrained fractional quadratic problem which is a non-convex problem. We turn the problem into an epigraph form so that we can
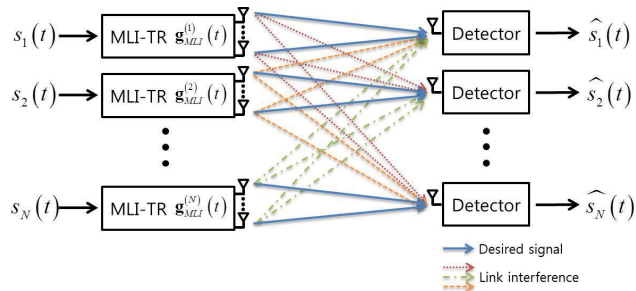

FIGURE 1. The block diagram of a ML-MISO system with the proposed MLI-TR prefilter.

apply the bisection method [41] to solve the optimization within the ε-optimal sense. Note that the found solution is a global optimal one as well. We also provide a method to find the boundaries of the bisection search along with the number of iterations needed for the solution to be settled.

This paper is organized as follows. In Section II, the system model of the multi-link MISO system is presented. In Section III, the optimization problem is formulated and a simple one-dimensional search-based scheme is proposed. In Section IV, the simulation results are illustrated and Section V gives the conclusions.

II. SYSTEM MODEL
We consider a multi-link MISO system that includes N transmitter and their intended receivers. Each transmitter has N_t antennas and each receiver is equipped with a single antenna. Assuming that one receiver is paired with a transmitter, the block diagram of an ML-MISO system is illustrated as Fig. 1. As shown in Fig. 1, each receiver experiences multi-link interference (MLI) from $N - 1$ transmitters. We assume that each transmitter knows the channel between it and all receivers by the channel reciprocity [12]. Note that this assumption is valid practically since the distance between the transmitter and the receiver is within a few meters, which is not long, in general, in the indoor wireless communication system [34].

In the indoor wireless communication, the multi-path channel is formed between transmitters and receivers. The channel remains static during a data burst, $100\mu s$ [34]. The CIR between the transmitter i and the receiver j is modelled as

$$\mathbf{h}_{i,j}(t) = \sum_{k=0}^{L-1} \mathbf{h}_{i,j}^{(k)} \delta(t - \tau_k), \qquad (1)$$

where L is the number of the channel components and $\mathbf{h}_{i,j}^{(k)}$ is a $1 \times N_t$ vector of the kth channel component with delay τ_k, which is the difference between the time of arrival with the earliest one, τ_0 [16].

The transmitted signal from the transmitter i to the receiver i is written as

$$\mathbf{x}_i(t) = \mathbf{g}_i(t) * s_i(t), \qquad (2)$$

where $*$ denotes convolution product, $\mathbf{g}_i(t)$ is a prefilter of the transmitter i and $s_i(t)$ indicates a transmit symbol for the receiver i with average power of 1. The prefilter, $\mathbf{g}_i(t)$ is represented as

$$\mathbf{g}_i(t) = \sum_{k=0}^{L-1} \mathbf{g}_i^{(k)} \delta(t - k\tau_s), \tag{3}$$

where $\mathbf{g}_i^{(k)}$ is the kth coefficient of the prefilter which is an $N_t \times 1$ vector and τ_s is a filter tap spacing [6]. Since the proposed prefilter is based on the TR prefilter, we set the number of the filter taps N. Thus, the received signal of the receiver i is

$$y_i(t) = \mathbf{h}_{i,i}(t) * \mathbf{x}_i(t) + \sum_{j=1, j \neq i}^{N} \mathbf{h}_{j,i}(t) * \mathbf{x}_j(t) + n_i(t), \tag{4}$$

where $n_i(t)$ denotes an additive zero-mean Gaussian noise with variance σ^2 at the receiver i. The received signal, $y_i(t)$ has the desired signal, ISI which is included in the first term of (4) and the MLI which is represented as the second term of (4). From (4), the equivalent CIR between the transmitter i and the receiver j can be written as

$$f_{i,j}(t) = \mathbf{h}_{i,j}(t) * \mathbf{g}_i(t)$$
$$= \sum_{k=0}^{2L-1} f_{i,j}^{(k)} \delta(t - k\tau_s), \tag{5}$$

where $f_{i,j}^{(k)}$ is the kth coefficient of $f_{i,j}(t)$. According to the channel length and the number of the filter taps, the length of the equivalent CIR is $2L - 1$.

Since the channel has multi-path components in the indoor wireless communication, the equation of the received signal is too complex to understand easily. Therefore, we use the Sylvester matrix form to simplify those equations. The equivalent CIR between the transmitter i and the receiver j is rewritten as

$$\mathbf{f}_{i,j} = \mathbf{H}_{i,j}\mathbf{g}_i$$

$$= \begin{bmatrix} \mathbf{h}_{i,j}^{(0)} & \mathbf{0} & & \mathbf{0} \\ \mathbf{h}_{i,j}^{(1)} & \mathbf{h}_{i,j}^{(0)} & & \vdots \\ \vdots & \mathbf{h}_{i,j}^{(1)} & \ddots & \mathbf{0} \\ \mathbf{h}_{i,j}^{(L-1)} & \vdots & \ddots & \mathbf{h}_{i,j}^{(0)} \\ \mathbf{0} & \mathbf{h}_{i,j}^{(L-1)} & & \mathbf{h}_{i,j}^{(1)} \\ \vdots & \mathbf{0} & \ddots & \vdots \\ \mathbf{0} & & & \mathbf{h}_{i,j}^{(L-1)} \end{bmatrix} \begin{bmatrix} \mathbf{g}_i^{(0)} \\ \mathbf{g}_i^{(1)} \\ \vdots \\ \mathbf{g}_i^{(L-1)} \end{bmatrix}$$

$$= \begin{bmatrix} f_{i,j}^{(0)} \\ f_{i,j}^{(1)} \\ \vdots \\ f_{i,j}^{(2L-1)} \end{bmatrix}, \tag{6}$$

where $\mathbf{H}_{i,j}$ is a $(2L-1) \times N_t L$ Sylvester matrix of the channel $\mathbf{h}_{i,j}(t)$, $\mathbf{g}_i$ is an $N_t L \times 1$ vector form of the prefilter $\mathbf{g}_i(t)$ and $\mathbf{f}_{i,j}$ is a $(2L-1) \times 1$ vector form of $f_{i,j}(t)$.

Using (6), the received signal can be rewritten as

$$\mathbf{y}_i = \sum_{j=1}^{N} \mathbf{H}_{j,i}\mathbf{g}_j s_j + \mathbf{n}_i = \mathbf{f}_{i,i}s_i + \sum_{j=1, j \neq i}^{N} \mathbf{f}_{j,i}s_j + \mathbf{n}_i, \tag{7}$$

where $\mathbf{n}_i$ and $\mathbf{y}_i$ are $(2L-1) \times 1$ vectors. In (7), $\mathbf{y}_i$ contains the delays of the transmitted signals, s_i, $i = 1, \cdots, N$.

A. CONVENTIONAL TR PREFILTER
In this subsection, we first introduce the conventional TR prefilter which is the base of the proposed prefilter [12]. The TR prefilter maximizes the received peak power and reduces the delay spread of the channel. The TR prefilter uses the time-reversed CIR as a prefilter which is represented by

$$\mathbf{h}_{i,i}^{TR} = \begin{bmatrix} \mathbf{h}_{i,i}^{(L-1)} & \mathbf{h}_{i,i}^{(L-2)} & \cdots & \mathbf{h}_{i,i}^{(0)} \end{bmatrix}^H. \tag{8}$$

Thus, the conventional TR prefilter of the transmitter i is represented as

$$\mathbf{g}_i^{TR} = \frac{1}{\left\| \mathbf{h}_{i,i}^{TR} \right\|} \mathbf{h}_{i,i}^{TR}, \tag{9}$$

where $\frac{1}{\left\| \mathbf{h}_{i,i}^{TR} \right\|}$ is used for normalization. Since the transmitted signal through the TR prefilter retraces the channel, the equivalent CIR, $\mathbf{f}_{i,i}$ is an autocorrelation of $\mathbf{h}_{i,i}(t)$. Therefore, strong temporal and spatial focusing is achieved for dense multipath channel. The ISI is mitigated by the temporal focusing and the MLI is decreased by the spatial focusing [22]. Nevertheless, the TR prefilter still suffers from the ISI because it considers only the received peak power maximization. The prefilter must take into consideration that the sidelobe of the received signal should be minimized. In addition, the MLI mitigation effect of the TR prefilter is an accompanying phenomenon. To sum up, the TR prefilter cannot control the interference excellently.

III. PROPOSED PREFILTER: MLI-TR PREFILTER
For a multi-link indoor wireless communication, we propose a prefilter which considers the sidelobe of the received signal and the leakage signal to other receivers in order to control the MLI and the ISI. Additionally, the proposed prefilter maximizes the received peak power like the conventional TR prefilter.

A. INTERFERENCE ANALYSIS
To design the prefilter, we analyze the interference of the received signal. At first, we find the desired signal which is from the transmitter i to the receiver i as

follows:

$$\mathbf{r}_{i,i} = \mathbf{H}_{i,i}\mathbf{g}_i s_i$$

$$= \begin{bmatrix} \mathbf{h}_{i,i}^{(0)} & \mathbf{0} & & \mathbf{0} \\ \mathbf{h}_{i,i}^{(1)} & \mathbf{h}_{i,i}^{(0)} & & \vdots \\ \vdots & \mathbf{h}_{i,i}^{(1)} & \ddots & \mathbf{0} \\ \mathbf{h}_{i,i}^{(L-1)} & \vdots & \ddots & \mathbf{h}_{i,i}^{(0)} \\ \mathbf{0} & \mathbf{h}_{i,i}^{(L-1)} & & \mathbf{h}_{i,i}^{(1)} \\ \vdots & \mathbf{0} & \ddots & \vdots \\ \mathbf{0} & & & \mathbf{h}_{i,i}^{(L-1)} \end{bmatrix} \begin{bmatrix} \mathbf{g}_i^{(0)} \\ \mathbf{g}_i^{(1)} \\ \vdots \\ \mathbf{g}_i^{(L-1)} \end{bmatrix} s_i. \tag{10}$$

In (10), we can find the main peak power of the desired signal as

$$P_{main,i} = \left| \mathbf{h}_{i,i}^{TR}\mathbf{g}_i \right|^2, \tag{11}$$

where $\mathbf{h}_{i,i}^{TR}$ represented in (8) is the Lth row of $\mathbf{H}_{i,i}$. Also, we can find the sidelobe of the desired signal that is the ISI of the transmitter i in (10). The sidelobe means the residual signal but the main peak of the desired signal. To remove the main peak from (10), we set the Lth row of $\mathbf{H}_{i,i}$ as zero vector as follows:

$$\tilde{\mathbf{H}}_{i,i} = \begin{bmatrix} \mathbf{h}_{i,i}^{(0)} & \mathbf{0} & \mathbf{0} & & \mathbf{0} \\ & \mathbf{h}_{i,i}^{(0)} & \mathbf{0} & & \\ \vdots & & \mathbf{h}_{i,i}^{(0)} & & \vdots \\ & \vdots & \vdots & \ddots & \\ \mathbf{h}_{i,i}^{(L-2)} & \mathbf{h}_{i,i}^{(L-3)} & \mathbf{h}_{i,i}^{(L-4)} & & \\ \mathbf{0} & \mathbf{0} & \mathbf{0} & & \mathbf{0} \\ \vdots & \mathbf{h}_{i,i}^{(L-1)} & \mathbf{h}_{i,i}^{(L-2)} & & \mathbf{h}_{i,i}^{(1)} \\ & \mathbf{0} & \mathbf{h}_{i,i}^{(L-1)} & & \vdots \\ \mathbf{0} & & \mathbf{0} & & \mathbf{h}_{i,i}^{(L-1)} \end{bmatrix}. \tag{12}$$

Thus, the power of the sidelobe can be written using $\tilde{\mathbf{H}}_{i,i}$ as

$$P_{sidelobe,i} = \left| \tilde{\mathbf{H}}_{i,i}\mathbf{g}_i \right|^2. \tag{13}$$

The proposed prefilter, so-called MLI-TR prefilter, considers the leakage power defined as the power of the undesired signal toward non-paired receivers. In order to design prefilter for each transmitter, it is ideal when the channel information between its own paired receiver and the all interfering links of is available to each transmitter, which is practically impossible. However, the transmitter can acquire the channel information between itself and the all receivers. Therefore, considering the leakage power from the transmitter rather than the interference power of its paired receiver, we propose a prefilter considering the leakage power which is expressed as

$$P_{leakage(i,j)} = \left| \mathbf{H}_{i,j}\mathbf{g}_i \right|^2, \tag{14}$$

where $P_{leakage(i,j)}$ represents the leakage power from the transmitter i to the receiver j.

To improve the performance of the prefilter, the proposed prefilter should consider the main peak power, the ISI and the MLI simultaneously. The signal power to sidelobe power ratio (SSR) is calculated as the ratio of the main peak power of the received signal to the sum power of the sidelobe [35], [36]. However, the SSR cannot represent the performance of the multi-link communication properly since it does not contain the MLI. In this paper, we introduce a new parameter to apply the leakage power - signal power to sidelobe power plus leakage power ratio (SSLR). As the leakage power is contained in the parameter, the SSLR can represent the performance of the multi-link communication system under limited channel information. Thus, the expression of the SSLR at the transmitter i is

$$SSLR_i = \frac{\left| \mathbf{h}_{i,i}^{TR}\mathbf{g}_i \right|^2}{\left| \tilde{\mathbf{H}}_{i,i}\mathbf{g}_i \right|^2 + \sum_{j=1, j \neq i}^{N} \left| \mathbf{H}_{i,j}\mathbf{g}_i \right|^2}. \tag{15}$$

As the SSLR is increased, the overall performance of the multi-link communication system is improved.

B. PROBLEM FORMULATION
The proposed MLI-TR prefilter maximizes the SSLR by controlling the coefficients of the prefilter using a weight matrix. That is, we control the coefficients of the conventional TR prefilter to design the weight matrix. The proposed prefilter with the weight matrix, $\mathbf{W}_i$ at the transmitter i is represented as

$$\mathbf{g}_i^{MLI} = \mathbf{W}_i \mathbf{h}_{i,i}^{TR}, \tag{16}$$

where $\mathbf{W}_i = \text{diag}\left[w_{i,1} \ w_{i,2} \cdots w_{i,(N_t L)} \right]$ is a diagonal matrix. Since the weight matrix maximizes the SSLR, the main peak power of the desired signal is maximized and the ISI and the MLI are minimized at the same time.

At the receiver i, the effective channels of desired link and interfering link from the transmitter j are expressed as

$$\mathbf{f}_{i,desired}^{MLI} = \mathbf{H}_{i,i}\mathbf{W}_i \mathbf{h}_{i,i}^{TR}$$

$$= \mathbf{H}_{i,i} diag\left(\mathbf{h}_{i,i}^{TR} \right) \begin{bmatrix} w_{i,1} \\ \vdots \\ w_{i,(N_t L)} \end{bmatrix} = \mathbf{H}_{i,i}\mathbf{D}_i^{TR}\mathbf{w}_i, \tag{17}$$

and

$$\mathbf{f}_{i,interference(j)}^{MLI} = \mathbf{H}_{j,i}\mathbf{W}_j \mathbf{h}_{j,j}^{TR}$$

$$= \mathbf{H}_{j,i} diag\left(\mathbf{h}_{j,j}^{TR} \right) \begin{bmatrix} w_{j,1} \\ \vdots \\ w_{j,(N_t L)} \end{bmatrix}$$

$$= \mathbf{H}_{j,i}\mathbf{D}_j^{TR}\mathbf{w}_j, \tag{18}$$

respectively, where $\mathbf{w}_i$ is a vector form of $\mathbf{W}_i$ and $\mathbf{D}_i^{TR}$ is a diagonal matrix form of $\mathbf{h}_{i,i}^{TR}$. The reason why we

manipulate the effective channel at the receiver i is that the SSLR can be represented by the fractional quadratic form as (19), where $\mathbf{Q}_{i,1} = \left(\mathbf{D}_i^{TR}\right)^H \mathbf{H}_{i,i}^H \mathbf{H}_{i,i} \mathbf{D}_i^{TR}$ and $\mathbf{Q}_{i,2} = \left(\mathbf{D}_i^{TR}\right)^H \left(\tilde{\mathbf{H}}_{i,i}^H \tilde{\mathbf{H}}_{i,i} + \sum_{j=1, j \neq i}^{N} \mathbf{H}_{i,j}^H \mathbf{H}_{i,j}\right) \mathbf{D}_i^{TR}$.

We assume that each transmitter uses same power like the conventional TR prefilter. So, the transmit power constraint is expressed as

$$\mathbf{w}_i^H \left(\mathbf{D}_i^{TR}\right)^H \mathbf{D}_i^{TR} \mathbf{w}_i = \mathbf{w}_i^H \mathbf{Q}_{i,3} \mathbf{w}_i = 1, \quad (20)$$

where $\mathbf{Q}_{i,3} = \left(\mathbf{D}_i^{TR}\right)^H \mathbf{D}_i^{TR}$.

To sum up, we want to find the weight matrix to maximize the SSLR using the limited channel information. Without the cooperation between transmitters, each transmitter designs the MLI-TR prefilter considering the leakage power. Therefore, the optimization problem for the MLI-TR prefilter of the transmitter i is

$$\max_{\mathbf{w}_i \in F} \frac{\mathbf{w}_i^H \mathbf{Q}_{i,1} \mathbf{w}_i}{\mathbf{w}_i^H \mathbf{Q}_{i,2} \mathbf{w}_i}$$
$$\text{subject to} \quad F = \left\{ \mathbf{w}_i \in \mathbb{R}^{N_t L \times 1} : \mathbf{w}_i^H \mathbf{Q}_{i,3} \mathbf{w}_i = 1 \right\}. \quad (21)$$

C. SOLVING THE OPTIMIZATION PROBLEM

The optimization problem (21) is a quadratically constrained fractional quadratic problem which is a non-convex problem because of the objective function. It is difficult to find an optimal solution of (21) since both the terms $\mathbf{Q}_{i,1}$ in the numerator of (21) and $\mathbf{Q}_{i,2}$ in the denominator of (21) are singular. Note that the singularity of these two matrices can be verified by the theorems in [37] with the properties about rank of the matrices, and some properties about the elementary row operations. Therefore, we cannot solve the problem (21) directly via the generalized eigenvalue problem [38], [39].

Nevertheless, we can find a global ε-optimal solution by converting the original optimization problem into a sequence of very simple convex optimization problems with a single parameter [40]. The ε-optimal solution of (21), $\mathbf{w}_i^*$ can be found by a simple one-dimensional search algorithm,

$$\frac{\mathbf{w}_i^{*H} \mathbf{Q}_{i,1} \mathbf{w}_i^*}{\mathbf{w}_i^{*H} \mathbf{Q}_{i,2} \mathbf{w}_i^*} \geq \max_{\mathbf{w}_i \in F} \frac{\mathbf{w}_i^H \mathbf{Q}_{i,1} \mathbf{w}_i}{\mathbf{w}_i^H \mathbf{Q}_{i,2} \mathbf{w}_i} - \varepsilon. \quad (22)$$

Observation 1: We can find simple observations in (21) as follows:
1. $\max\limits_{\mathbf{w}_i \in F} \frac{\mathbf{w}_i^H \mathbf{Q}_{i,1} \mathbf{w}_i}{\mathbf{w}_i^H \mathbf{Q}_{i,2} \mathbf{w}_i} \geq \alpha.$
2. $\max\limits_{\mathbf{w}_i \in F} \left\{ \mathbf{w}_i^H \mathbf{Q}_{i,1} \mathbf{w}_i - \alpha \mathbf{w}_i^H \mathbf{Q}_{i,2} \mathbf{w}_i \right\} \geq 0.$

From these observations, we can convert the original optimization problem (21) to the epigraph form as follows [41]:

$$\max_{\mathbf{w}_i \in F} \alpha$$
$$\text{subject to} \quad \frac{\mathbf{w}_i^H \mathbf{Q}_{i,1} \mathbf{w}_i}{\mathbf{w}_i^H \mathbf{Q}_{i,2} \mathbf{w}_i} - \alpha \geq 0,$$
$$F = \left\{ \mathbf{w}_i \in \mathbb{R}^{N_t L \times 1} : \mathbf{w}_i^H \mathbf{Q}_{i,3} \mathbf{w}_i = 1 \right\}. \quad (23)$$

Therefore, we can find a solution by the bisection method in Table 1 which is expressed as

$$\mathbf{w}_i^* \in \arg\max_{\mathbf{w}_i \in F} \left\{ \mathbf{w}_i^{*H} \mathbf{Q}_{i,1} \mathbf{w}_i^* - u_k^* \mathbf{w}_i^{*H} \mathbf{Q}_{i,2} \mathbf{w}_i^* \right\}. \quad (24)$$

The bisection method iterates until the gap between the lower bound and the upper bound is less than ε. Thus, as β_k is close to 0, α_k is going to the maximum value and then the solution, $\mathbf{w}_i$ from the subproblem, (1) is the optimal solution of (23). Since we find a global optimal solution of the subproblem, (1), we can find the ε-optimal solution [40].

It is difficult to solve the subproblem (1), because it is a nonconvex problem. Thus, we use $\mathbf{s}_i = \mathbf{Q}_{i,3}^{1/2} \mathbf{w}_i$ for simplification of the constraint as

$$\mathbf{w}_i^H \mathbf{Q}_{i,3} \mathbf{w}_i = \|\mathbf{s}_i\|^2 = 1. \quad (26)$$

The constraint converts to the Euclidean norm. Moreover, the objective function of the subproblem can be converted to the quadratic function as follows:

$$\mathbf{w}_i^H \mathbf{Q}_{i,1} \mathbf{w}_i - \alpha_k \mathbf{w}_i^H \mathbf{Q}_{i,2} \mathbf{w}_i$$
$$= \mathbf{s}_i^H \left\{ \left(\mathbf{Q}_{i,3}^{-\frac{1}{2}} \right)^H \left(\mathbf{Q}_{i,1} - \alpha_k \mathbf{Q}_{i,2} \right) \mathbf{Q}_{i,3}^{-\frac{1}{2}} \right\} \mathbf{s}_i$$
$$= \mathbf{s}_i^H \tilde{\mathbf{Q}}_i \mathbf{s}_i, \quad (27)$$

$$SSLR_i = \frac{\mathbf{w}_i^H \left(\mathbf{D}_i^{TR}\right)^H \mathbf{H}_{i,i}^H \mathbf{H}_{i,i} \mathbf{D}_i^{TR} \mathbf{w}_i}{\mathbf{w}_i^H \left(\mathbf{D}_i^{TR}\right)^H \tilde{\mathbf{H}}_{i,i}^H \tilde{\mathbf{H}}_{i,i} \mathbf{D}_i^{TR} \mathbf{w}_i + \sum\limits_{j=1, j \neq i}^{N} \mathbf{w}_i^H \left(\mathbf{D}_i^{TR}\right)^H \mathbf{H}_{i,j}^H \mathbf{H}_{i,j} \mathbf{D}_i^{TR} \mathbf{w}_i}$$
$$= \frac{\mathbf{w}_i^H \left[\left(\mathbf{D}_i^{TR}\right)^H \mathbf{H}_{i,i}^H \mathbf{H}_{i,i} \mathbf{D}_i^{TR} \right] \mathbf{w}_i}{\mathbf{w}_i^H \left[\left(\mathbf{D}_i^{TR}\right)^H \left(\tilde{\mathbf{H}}_{i,i}^H \tilde{\mathbf{H}}_{i,i} + \sum\limits_{j=1, j \neq i}^{N} \mathbf{H}_{i,j}^H \mathbf{H}_{i,j} \right) \mathbf{D}_i^{TR} \right] \mathbf{w}_i}$$
$$= \frac{\mathbf{w}_i^H \mathbf{Q}_{i,1} \mathbf{w}_i}{\mathbf{w}_i^H \mathbf{Q}_{i,2} \mathbf{w}_i}, \quad (19)$$

TABLE 1. Bisection method for (23).

The Bisection Method

Step 1. Set the initial bound: the lower bound is $l_0 = m$ and the upper bound is $u_0 = M$.

Step 2. For every $k \geq 1$
    (a) Define $\alpha_k = \frac{u_{k-1}+l_{k-1}}{2}$.
    (b) Calculate β_k.

$$\beta_k = \max_{\mathbf{w}_i \in F} \left\{ \mathbf{w}_i^H \mathbf{Q}_{i,1} \mathbf{w}_i - \alpha_k \mathbf{w}_i^H \mathbf{Q}_{i,2} \mathbf{w}_i \right\} \quad (25)$$

    (b-1) If $\beta_k < 0$, then define $l_k = \alpha_k$, $u_k = u_{k-1}$.
    (b-2) If $\beta_k \geq 0$, then define $l_k = l_{k-1}$, $u_k = \alpha_k$

Step 3. If $u_k - l_k \leq \varepsilon$, stop iteration and get $\mathbf{w}_i^*$ with u_k^* using Eq. (23). If not, go to Step 2.

where $\tilde{\mathbf{Q}}_i = \left(\mathbf{Q}_{i,3}^{-\frac{1}{2}} \right)^H \left(\mathbf{Q}_{i,1} - \alpha_k \mathbf{Q}_{i,2} \right) \mathbf{Q}_{i,3}^{-\frac{1}{2}}$. Therefore, the subproblem is manipulated as

$$\max_{\|\mathbf{s}_i\|^2=1} \left\{ \mathbf{s}_i^H (\tilde{\mathbf{Q}}_i) \mathbf{s}_i \right\}, \quad (28)$$

which is a convex optimization problem. We can solve this optimization problem using the Lagrangian's method [41], where the proof is represented in Appendix A. The initial upper bound and lower bound M and m are given by

$$M = \frac{\lambda_{\max}(\mathbf{Q}_{i,1}) \lambda_{\max}(\mathbf{Q}_{i,3})}{\lambda_{\min}(\mathbf{Q}_{i,3}) \lambda_{\min}(\mathbf{Q}_{i,2})}. \quad (29)$$

$$m = -M. \quad (30)$$

The derivation of initial bounds is represented in Appendix B. As we set the initial bound, we can calculate the number of the iteration of the bisection method as follows:

Proposition 1: The bisection algorithm ends after $\left\lceil \ln\left(\frac{M-m}{\varepsilon}\right) \middle/ \ln 2 \right\rceil$ iterations with an output $\mathbf{w}^*$ that is an optimal ε-solution of (21).

Proof: The length of initial bound is $u_0 - l_0 = M - m$. By the definition of the u_k and l_k, we can find the relationship for every k as $u_k - l_k = \frac{1}{2}(u_{k-1} - l_{k-1})$. Thus, this relationship is established,

$$u_k - l_k = (M - m)\left(\frac{1}{2}\right)^k. \quad (31)$$

Since the iteration ends when $u_k - l_k \leq \varepsilon$, the number of the iteration k^* has

$$(M - m)\left(\frac{1}{2}\right)^{k^*} \leq \varepsilon, \quad (32)$$

which is equivalent to $k^* \geq \left\lceil \ln\left(\frac{M-m}{\varepsilon}\right) \middle/ \ln(2) \right\rceil$. $\qquad \square$

In addition, note that only $2L - 1$ equations are considered for the proposed MLI-TR prefilter while $2L + L_E - 2$ equations are required for the conventional ETR prefilter [21], where L_E denotes a length of an equalizer added in the transmitter, which results in high computational complexity for sufficient suppression of the inter-symbol interference.

TABLE 2. Multipath channel characteristics of IEEE 802.15.3a channel model [42].

	CM1	CM2	CM3
Mean excess delay (nsec)	5.0	9.9	15.9
RMS delay (nsec)	5	8	15
Channel energy mean	-0.4	-0.5	0
Channel energy standard	2.9	3.1	3.1
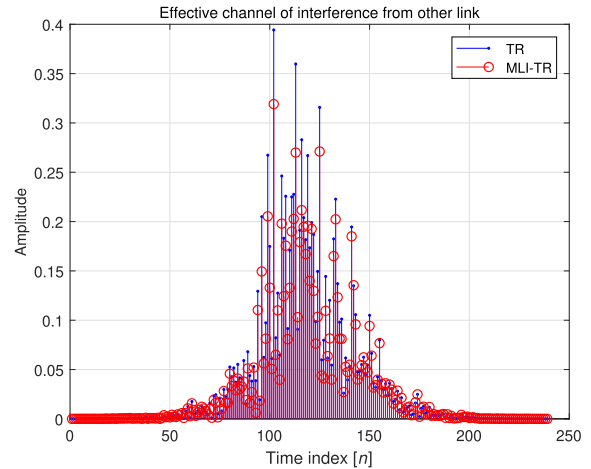
FIGURE 2. Comparison of other link interferences.

IV. SIMULATION RESULTS

We compare the performance of the proposed MLI-TR prefilter with that of the conventional TR prefilter and the ETR prefilter. We consider the channel model in IEEE 802.15.3a [42] which is the indoor wireless channel for short ranges and high data rate. Especially, we use the channel model (CM) 1, 2 and the CM3 and their characteristics are represented in Table 2. The CM1 is based on line of sight (LOS) channel measurements in a small room (0-4m). In case of CM2 and CM3, they are based on non line of sight (NLOS) channel measurements in a small room (0-4m) and large room (4-10m), respectively. There are N links between N transmitters and N receivers. The transmitters have 4 antennas and the receivers have a single antenna. We use the QPSK modulation and vary the symbol duration T_s and the number of links to observe the interference effect.

In Fig. 2, we represent the impulse response of the leakage signal power to other links when there are 2 links in the network. Since the objective of the MLI-TR prefilter is to reduce the leakage interference to other links, the power of the leakage signal of the conventional TR prefilter is larger than that of the MLI-TR prefilter. Thus, the MLI-TR prefilter improves the performance by reducing the leakage signal.

We compare the SSLR of the conventional TR prefilter and the MLI-TR prefilter in Fig. 3 and Fig. 4. Though the number of links is increased, the SSLR of the MLI-TR prefilter is higher than that of the conventional TR prefilter as in Fig. 3. In Fig. 4, we represent the increasing rate of the SSLR of the MLI-TR prefilter compared to the TR prefilter.
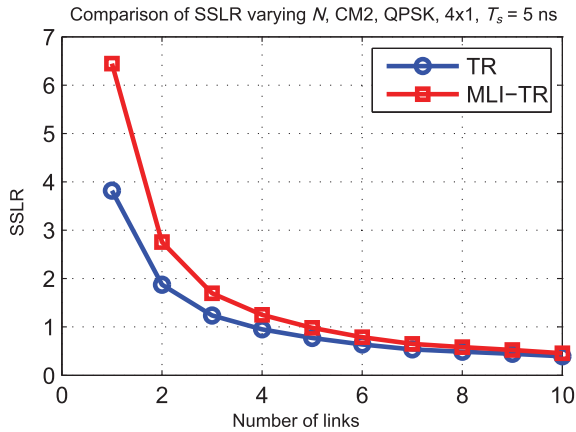
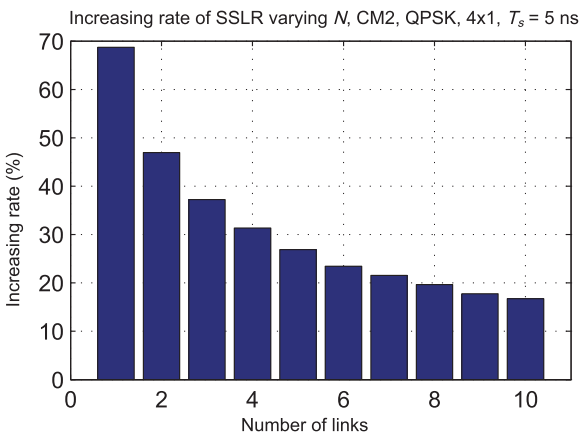**FIGURE 3.** Comparison of the SSLR for various *N*.

FIGURE 4. Increasing rates of the SSLR for various *N*.

FIGURE 5. Comparison of BER for the CM1 with 2 links and various T_S.

FIGURE 6. Comparison of BER for the CM2 with 2 links and various T_S.

The increasing rate of the SSLR is decreased as the number of links is increased because the leakage signal between links occurs seriously. This means that MLI and ISI would be greatly affected by increasing the number of links in the multi-link system.

Considering that the MLI-TR prefilter can enhance the effective desired signal power compared to that of the conventional TR prefilter, we can use BER as well as SSLR as a performance of multi-link system to show the effectiveness of the MLI-TR prefilter. As shown in Fig. 5, the BER performances of the conventional TR prefilter, the ETR prefilter and the MLI-TR prefilter in the CM1 are compared. There are 2 links in the network and the symbol duration is 1ns, 5ns or 10ns. Since the ISI is increased as the symbol duration is short, the BER performances of all prefilters are degraded. Comparing the conventional TR prefilter and the ETR prefilter, in the case of the short symbol duration, BER performance of the ETR prefilter is better because the ISI has a large influence. However, the BER performance of the MLI-TR prefilter is better than that of other prefilters in every symbol duration by maximizing the SSLR.

In Fig. 6 and Fig. 7, we compare the BER performances of the conventional TR prefilter, the ETR prefilter and the
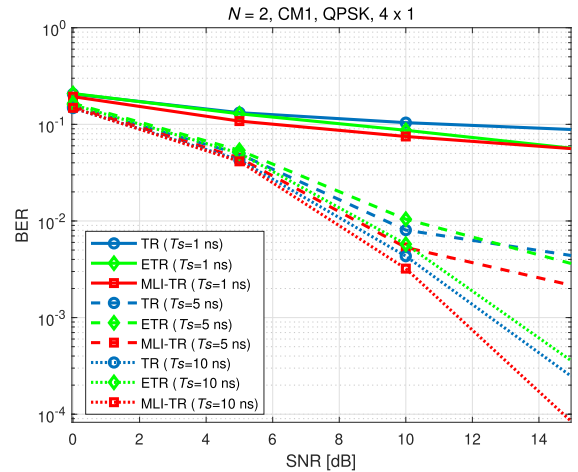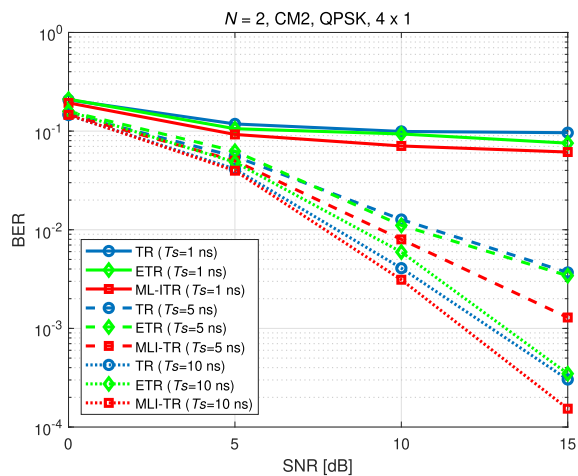
MLI-TR prefilter in the CM2 and CM3, respectively. Since CM2 and CM3 are based on NLOS channel measurement, the delay spread effect of the CM2 and CM3 are larger than the CM1. However, the BER performance of the MLI-TR prefilter is improved by maximizing the SSLR. Moreover, compared with other prefilters, the MLI-TR prefilter exhibits the best BER performance for every symbol duration. Therefore, we can conclude that the MLI-TR prefilter is robust to the delay spread.

In Fig. 8 and Fig. 9, we compare the BER performances of two prefilters in the CM2 when the symbol duration is 5ns and 10ns with various numbers of links (3, 5, 7 links). As the number of links is increased, the BER performances of both prefilters are degraded because the MLI is significantly increased. However, the MLI-TR prefilter has better BER performance in overall SNR range because the MLI-TR prefilter reduces the MLI and the ISI at the same time. To show the effect of the MLI reduction, we set the symbol duration to be 10ns in Fig. 9: the effect of the ISI is very small. When the ISI is small, the MLI-TR prefilter has better BER performance
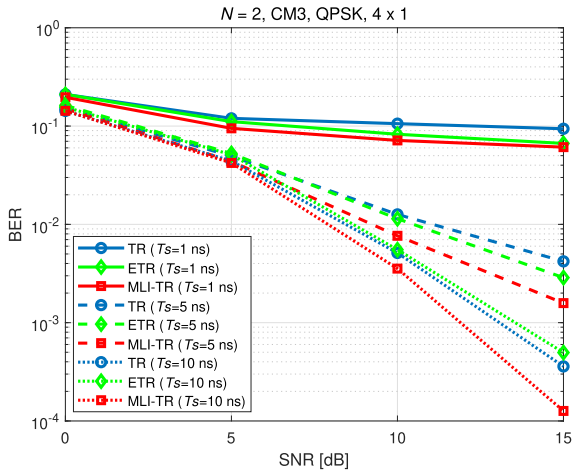
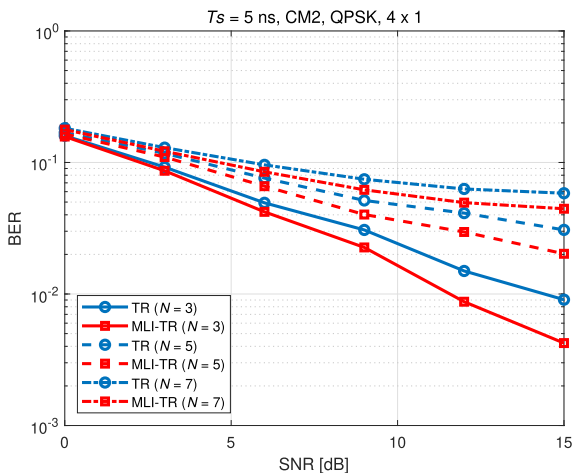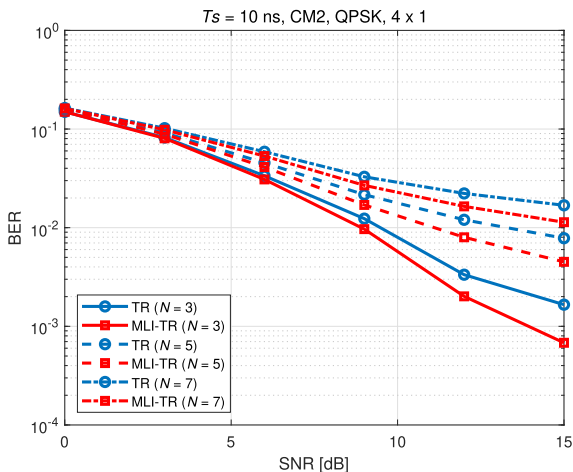**FIGURE 7.** Comparison of BER for the CM3 with 2 links and various T_s.

FIGURE 8. Comparison of BER for the CM2 with T_s = 5 ns and various N.

FIGURE 9. Comparison of BER for the CM2 with T_s = 10 ns and various N.

than the TR prefilter. That is, the MLI-TR prefilter can control the leakage signal.

V. CONCLUSION
We propose the MLI-TR prefilter for multi-link indoor wireless communication. The MLI-TR prefilter reduces the MLI and the ISI at the same time by controlling the leakage signal

to other links. We define the SSLR to consider the main signal, the ISI and the MLI simultaneously. The MLI-TR prefilter maximizes the SSLR to maximize the main peak power and minimize the ISI and the MLI.

To maximize the SSLR, we design the optimization problem and find the ε-optimal solution as the MLI-TR prefilter. Simulation results show that the MLI-TR prefilter improves the BER performance. Especially, we presented the leakage signal is controlled by the MLI-TR prefilter efficiently and therefore can be applied to the multi-link indoor wireless communication systems. A further extension of the efficient ISI/MLI management based on SSLR maximization would be considered in a multi-link systems with the transmitters enabled with serving multiple devices for future work.

APPENDIX A
The Lagrangian function of this problem is

$$l\left(\mathbf{s}_i, \lambda\right) = \mathbf{s}_i^H(\tilde{\mathbf{Q}}_i)\mathbf{s}_i + \lambda(1 - \mathbf{s}_i^H\mathbf{s}_i). \tag{33}$$

Applying the Lagrangian condition yields

$$D_{\mathbf{s}_i}l\left(\mathbf{s}_i, \lambda\right) = 2\mathbf{s}_i^H\tilde{\mathbf{Q}}_i - 2\lambda\mathbf{s}_i^H = \mathbf{0}^T. \tag{34}$$

$$D_\lambda l\left(\mathbf{s}_i, \lambda\right) = 1 - \mathbf{s}_i^H\mathbf{s}_i = 0 \tag{35}$$

The equation (34) can be represented as

$$(\lambda\mathbf{I} - \tilde{\mathbf{Q}}_i)\mathbf{s}_i = \mathbf{0}, \tag{36}$$

equivalently,

$$\tilde{\mathbf{Q}}_i\mathbf{s}_i = \lambda\mathbf{s}_i. \tag{37}$$

Therefore, the solution is an eigenvector of $\tilde{\mathbf{Q}}_i$ and the Lagrangian multiplier is the corresponding eigenvalue. Since the optimum value λ^* maximizes the objective function, the value λ^* is a maximum eigenvalue of $\tilde{\mathbf{Q}}_i$ and the optimal solution, $\mathbf{s}_i^*$ is the eigenvector of $\tilde{\mathbf{Q}}_i$ corresponding to λ^*.

To check the second-order sufficient conditions (SOSC), we first compute the Hessian matrix of the Lagrangian function as

$$L(\mathbf{s}_i^*, \lambda^*) = 2\tilde{\mathbf{Q}}_i - 2\lambda^*\mathbf{I}, \tag{38}$$

which is positive definite. The Lagrangian condition is also satisfied

$$D_{\mathbf{s}_i}l(\mathbf{s}_i^*, \lambda^*) = 2\mathbf{s}_i^{*H}\tilde{\mathbf{Q}}_i - 2\lambda^*\mathbf{s}_i^{*H} = \mathbf{0}^T. \tag{39}$$

Therefore, the solution $\mathbf{s}_i^*$ is an optimal solution of the subproblem.

APPENDIX B
The bisection method needs the initial bound to find a solution. As we set the initial bound close to the solution, the iteration could be finished quickly. Thus, how we choose the lower and upper bounds m and M, respectively, is important. From the constraint (20), we can get an inequality of $\mathbf{w}_i^H\mathbf{w}_i$ using the Rayleigh-Ritz theorem as follows [43]:

$$\lambda_{\min}\left(\mathbf{Q}_{i,3}\right) \le \frac{\mathbf{w}_i^H\mathbf{Q}_{i,3}\mathbf{w}_i}{\mathbf{w}_i^H\mathbf{w}_i} = \frac{1}{\mathbf{w}_i^H\mathbf{w}_i} \le \lambda_{\max}\left(\mathbf{Q}_{i,3}\right)$$

$$\Rightarrow \frac{1}{\lambda_{\max}\left(\mathbf{Q}_{i,3}\right)} \leq \mathbf{w}_i^H \mathbf{w}_i \leq \frac{1}{\lambda_{\min}\left(\mathbf{Q}_{i,3}\right)} \quad (40)$$

where $\lambda_{\min}\left(\mathbf{A}\right)$ is a minimum eigenvalue of $\mathbf{A}$ and $\lambda_{\max}\left(\mathbf{A}\right)$ is a maximum eigenvalue of $\mathbf{A}$. Note that the eigenvalues of $\mathbf{Q}_{i,1}$, $\mathbf{Q}_{i,2}$, and $\mathbf{Q}_{i,3}$ are positive, since those are Hermitian and positive definite matrices. So, we can find inequalities of $\mathbf{Q}_{i,1}$ and $\mathbf{Q}_{i,2}$ using the Rayleigh-Ritz theorem as follows:

$$\lambda_{\min}\left(\mathbf{Q}_{i,1}\right)\mathbf{w}_i^H\mathbf{w}_i \leq \mathbf{w}_i^H\mathbf{Q}_{i,1}\mathbf{w}_i$$
$$= 1$$
$$\leq \lambda_{\max}\left(\mathbf{Q}_{i,1}\right)\mathbf{w}_i^H\mathbf{w}_i, \quad (41)$$
$$\lambda_{\min}\left(\mathbf{Q}_{i,2}\right)\mathbf{w}_i^H\mathbf{w}_i \leq \mathbf{w}_i^H\mathbf{Q}_{i,2}\mathbf{w}_i$$
$$= 1$$
$$\leq \lambda_{\max}\left(\mathbf{Q}_{i,2}\right)\mathbf{w}_i^H\mathbf{w}_i. \quad (42)$$

From (40) and (41), we can merge two inequalities as

$$\frac{\lambda_{\min}\left(\mathbf{Q}_{i,1}\right)}{\lambda_{\max}\left(\mathbf{Q}_{i,3}\right)} \leq \mathbf{w}_i^H\mathbf{Q}_{i,1}\mathbf{w}_i \leq \frac{\lambda_{\max}\left(\mathbf{Q}_{i,1}\right)}{\lambda_{\min}\left(\mathbf{Q}_{i,3}\right)}. \quad (43)$$

Also, we can merge two inequalities (40) and (42) as

$$\frac{\lambda_{\min}\left(\mathbf{Q}_{i,2}\right)}{\lambda_{\max}\left(\mathbf{Q}_{i,3}\right)} \leq \mathbf{w}_i^H\mathbf{Q}_{i,2}\mathbf{w}_i \leq \frac{\lambda_{\max}\left(\mathbf{Q}_{i,2}\right)}{\lambda_{\min}\left(\mathbf{Q}_{i,3}\right)}. \quad (44)$$

Based on these inequalities, (43) and (44), we set the initial bound from this inequality,

$$\left|\frac{\mathbf{w}_i^H\mathbf{Q}_{i,1}\mathbf{w}_i}{\mathbf{w}_i^H\mathbf{Q}_{i,2}\mathbf{w}_i}\right| \leq \frac{\max\left|\mathbf{w}_i^H\mathbf{Q}_{i,1}\mathbf{w}_i\right|}{\min\left|\mathbf{w}_i^H\mathbf{Q}_{i,2}\mathbf{w}_i\right|}$$
$$\leq \frac{\lambda_{\max}\left(\mathbf{Q}_{i,1}\right)}{\lambda_{\min}\left(\mathbf{Q}_{i,3}\right)} \bigg/ \frac{\lambda_{\min}\left(\mathbf{Q}_{i,2}\right)}{\lambda_{\max}\left(\mathbf{Q}_{i,3}\right)}$$
$$= \frac{\lambda_{\max}\left(\mathbf{Q}_{i,1}\right)\lambda_{\max}\left(\mathbf{Q}_{i,3}\right)}{\lambda_{\min}\left(\mathbf{Q}_{i,3}\right)\lambda_{\min}\left(\mathbf{Q}_{i,2}\right)}. \quad (45)$$

Therefore, the upper bound is

$$M = \frac{\lambda_{\max}\left(\mathbf{Q}_{i,1}\right)\lambda_{\max}\left(\mathbf{Q}_{i,3}\right)}{\lambda_{\min}\left(\mathbf{Q}_{i,3}\right)\lambda_{\min}\left(\mathbf{Q}_{i,2}\right)}. \quad (46)$$

The lower bound is

$$m = -M. \quad (47)$$

REFERENCES

[1] S. R. Wood and R. Aiello, *Essentials of UWB*. Cambridge, U.K.: Cambridge Univ. Press, 2008.

[2] J. R. Foerster, "The effects of multipath interference on the performance of UWB systems in an indoor wireless channel," in *Proc. IEEE VTS 53rd Veh. Technol. Conf., Spring*, Rhodes, Greece, vol. 2, May 2001, pp. 1179–1180.

[3] K. Popovski, B. J. Wysocki, and T. A. Wysocki, "Modelling and comparative performance analysis of a time-reversed UWB system," *EURASIP J. Wireless Commun. Netw.*, vol. 2007, no. 1, Dec. 2007, Art. no. 071610.

[4] K. Witrisal, G. Leus, G. J. M. Janssen, M. Pausini, F. Troesch, T. Zasowski, and J. Romme, "Noncoherent ultra-wideband systems," *IEEE Signal Process. Mag.*, vol. 26, no. 4, pp. 48–66, Jul. 2009.

[5] Y.-L. Chao and R. A. Scholtz, "Optimal and suboptimal receivers for ultra-wideband transmitted reference systems," in *Proc. IEEE Global Telecommun. Conf. (GLOBECOM)*, San Francisco, CA, USA, vol. 2, Dec. 2003, pp. 759–763.

[6] N. Guo, R. C. Qiu, and B. M. Sadler, "An ultra-wideband autocorrelation demodulation scheme with low-complexity time reversal enhancement," in *Proc. IEEE Mil. Commun. Conf. (MILCOM)*, Atlantic City, NJ, USA, Oct. 2005, pp. 3066–3072.

[7] N. Guo and R. C. Qiu, "Improved autocorrelation demodulation receivers based on multiple-symbol detection for UWB communications," *IEEE Trans. Wireless Commun.*, vol. 5, no. 8, pp. 2026–2031, Aug. 2006.

[8] Y. Souilmi and R. Knopp, "On the achievable rates of ultra-wideband PPM with non-coherent detection in multipath environments," in *Proc. IEEE Int. Conf. Commun. (ICC)*, Anchorage, AK, USA, May 2003, pp. 3530–3534.

[9] M. E. Sahin, I. Guvenc, and H. Arslan, "Optimization of energy detector receivers for UWB systems," in *Proc. IEEE 61st Veh. Technol. Conf. (VTC) Spring*, Stockholm, Sweden, vol. 2, May 2005, pp. 1386–1390.

[10] A. M. Fouladgar, O. Simeone, O. Sahin, P. Popovski, and S. Shamai, "Joint interference alignment and bi-directional scheduling for MIMO two-way multi-link networks," in *Proc. IEEE Int. Conf. Commun.*, Washington, DC, USA, Jun. 2015, pp. 4126–4131.

[11] I. Aykin and M. Krunz, "Proactive sensing and interference mitigation in multi-link satellite networks," in *Proc. IEEE Global Commun. Conf. (GLOBECOM)*, Dec. 2016, pp. 1–6.

[12] R. C. Qiu, C. Zhou, N. Guo, and J. Q. Zhang, "Time reversal with MISO for ultrawideband communications: Experimental results," *IEEE Antennas Wireless Propag. Lett.*, vol. 5, pp. 269–273, May 2006.

[13] G. F. Edelmann, H. C. Song, S. Kim, W. S. Hodgkiss, W. A. Kuperman, and T. Akal, "Underwater acoustic communications using time reversal," *IEEE J. Ocean. Eng.*, vol. 30, no. 4, pp. 852–864, Oct. 2005.

[14] N. Guo, B. Sadler, and R. Qiu, "Reduced-complexity UWB time-reversal techniques and experimental results," *IEEE Trans. Wireless Commun.*, vol. 6, no. 12, pp. 4221–4226, Dec. 2007.

[15] T. Wang and T. Lv, "Canceling interferences for high data rate time reversal MIMO UWB system: A precoding approach," *EURASIP J. Wireless Commun. Netw.*, vol. 2011, no. 1, Dec. 2011, 959478.

[16] C. Zhou, N. Guo, and R. Caiming Qiu, "Time-reversed ultra-wideband (UWB) multiple input multiple output (MIMO) based on measured spatial channels," *IEEE Trans. Veh. Technol.*, vol. 58, no. 6, pp. 2884–2898, Jul. 2009.

[17] H. Tuan Nguyen, J. B. Andersen, G. F. Pedersen, P. Kyritsi, and P. C. F. Eggers, "Time reversal in wireless communications: A measurement-based investigation," *IEEE Trans. Wireless Commun.*, vol. 5, no. 8, pp. 2242–2252, Aug. 2006.

[18] D. Wang, L. G. Jiang, and C. He, "A MIMO transceiver scheme using TR-STBC for single-carrier UWB communications with frequency domain equalization," in *Proc.IEEE 2nd Int. Conf. Commun. Netw. China (CHINACOM)*, Shanghai, China, Aug. 2007, pp. 1142–1146.

[19] T. Strohmer, M. Emami, J. Hansen, G. Papanicolaou, and A. J. Paulraj, "Application of time-reversal with MMSE equalizer to UWB communications," in *Proc. IEEE Global Telecommun. Conf.*, Dallas, TX, USA, Nov. 2004, pp. 3123–3127.

[20] M. Yoon and C. Lee, "An improved TR prefilter for SSR maximization in indoor wireless communication system," *Wireless Pers. Commun.*, vol. 90, no. 3, pp. 1519–1532, Oct. 2016.

[21] C. A. Viteri-Mera and F. L. Teixeira, "Equalized time reversal beamforming for frequency-selective indoor MISO channels," *IEEE Access*, vol. 5, pp. 3944–3957, 2017.

[22] I. H. Naqvi, A. Khaleghi, and G. El Zein, "Multiuser time reversal UWB communication system: A modified transmission approach," in *Proc. IEEE 20th Int. Symp. Pers., Indoor Mobile Radio Commun. (PIMRC)*, Tokyo, Japan, Sep. 2009, pp. 2671–2675.

[23] F. Han, Y.-H. Yang, B. Wang, Y. Wu, and K. J. R. Liu, "Time-reversal division multiple access over multi-path channels," *IEEE Trans. Commun.*, vol. 60, no. 7, pp. 1953–1965, Jul. 2012.

[24] F. Han and K. J. R. Liu, "A multiuser TRDMA uplink system with 2D parallel interference cancellation," *IEEE Trans. Commun.*, vol. 62, no. 3, pp. 1011–1022, Mar. 2014.

[25] Y. Han, Y. Chen, B. Wang, and K. J. R. Liu, "Time-reversal massive multipath effect: A single-antenna 'massive MIMO' solution," *IEEE Trans. Commun.*, vol. 64, no. 8, pp. 3382–3394, Aug. 2014.

[26] C. A. Viteri-Mera, F. L. Teixeira, and K. Sainath, "Interference-nulling time-reversal beamforming for mm-Wave massive MIMO systems," in *Proc. IEEE Int. Conf. Microw., Commun., Antennas Electron. Syst. (COMCAS)*, Nov. 2015, pp. 1–5.

[27] D. Dupleich, S. Haefner, R. Muller, C. Schneider, J. Luo, and R. Thoma, "Real-field performance of hybrid MISO time reversal multi-beam beamformer at mm-waves," in *Proc. 11th Eur. Conf. Antennas Propag. (EUCAP)*, Paris, France, Mar. 2017, pp. 448–452.

[28] L. Wang, R. Li, C. Cao, and G. L. Stuber, "SNR analysis of time reversal signaling on target and unintended receivers in distributed transmission," *IEEE Trans. Commun.*, vol. 64, no. 5, pp. 2176–2191, May 2016.

[29] H.-V. Tran, G. Kaddoum, H. Tran, and E.-K. Hong, "Downlink power optimization for heterogeneous networks with time reversal-based transmission under backhaul limitation," *IEEE Access*, vol. 5, pp. 755–770, 2017.

[30] K. Amnatchotiphan, "Physical-layer security performance of MISO time-reversal ultra-wideband systems," in *Proc. Photon. Electromagn. Res. Symp. Fall (PIERS-FALL)*, Xiamen, China, Dec. 2019, pp. 493–499.

[31] Y. Chen, F. Han, Y.-H. Yang, H. Ma, Y. Han, C. Jiang, H.-Q. Lai, D. Claffey, Z. Safar, and K. J. R. Liu, "Time-reversal wireless paradigm for green Internet of Things: An overview," *IEEE Internet Things J.*, vol. 1, no. 1, pp. 81–98, Feb. 2014.

[32] Z. He, H. Ishikawa, R. Nakamura, and A. Kajiwara, "ICI of time-reversal UWB-IR communication," in *Proc. IEEE Topical Conf. Wireless Sensors Sensor Netw. (BioWireleSS)*, Austin, TX, USA, Jan. 2013, pp. 109–111.

[33] Y.-H. Yang, B. Wang, W. S. Lin, and K. J. R. Liu, "Near-optimal waveform design for sum rate optimization in time-reversal multiuser downlink systems," *IEEE Trans. Wireless Commun.*, vol. 12, no. 1, pp. 346–357, Jan. 2013.

[34] A. F. Molisch, J. R. Foerster, and M. Pendergrass, "Channel models for ultrawideband personal area networks," *IEEE Wireless Commun.*, vol. 10, no. 6, pp. 14–21, Dec. 2003.

[35] M.-S. Kim, M. Yoon, and C. Lee, "Performance analysis of a frequency-domain Equal-Gain-Combining time-reversal scheme for distributed antenna systems," *IEEE Commun. Lett.*, vol. 16, no. 9, pp. 1454–1457, Sep. 2012.

[36] M. Yoon and C. Lee, "A TR-MISI serial prefilter for robustness to ISI and noise in indoor wireless communication system," *IEEE Signal Process. Lett.*, vol. 21, no. 4, pp. 386–389, Apr. 2014.

[37] A. Howard and C. B. Robert, *Contemporary Linear Algebra*. Hoboken, NJ, USA: Wiley, 2003.

[38] A. Tarighat, M. Sadek, and A. H. Sayed, "A multi user beamforming scheme for downlink MIMO channels based on maximizing signal-to-leakage ratios," in *Proc. IEEE Int. Conf. Acoust., Speech, Signal Process.*, Philadelphia, PA, USA, Mar. 2005, pp. 1129–1132.

[39] M. Sadek, A. Tarighat, and A. H. Sayed, "Active antenna selection in multiuser MIMO communications," *IEEE Trans. Signal Process.*, vol. 55, no. 4, pp. 1498–1510, Apr. 2007.

[40] A. Beck, A. Ben-Tal, and M. Teboulle, "Finding a global optimal solution for a quadratically constrained fractional quadratic problem with applications to the regularized total least squares," *SIAM J. Matrix Anal. Appl.*, vol. 28, no. 2, pp. 425–445, Jan. 2006.

[41] S. Boyd and L. Vandenberghe, *Convex Optimization*. Cambridge, U.K.: Cambridge Univ. Press, 2004.

[42] *Channel Modeling Sub-Committee Report Final*, IEEE Standard P802.15 WPANs, 2012.

[43] R. A. Horn and C. R. Johnson, *Matrix Analysis*. Cambridge, U.K.: Cambridge Univ. Press, 1990.

MISUN YOON received the B.S. and Ph.D. degrees in electronic engineering from Yonsei University, Seoul, South Korea, in 2008 and 2015, respectively. She has been a Senior Engineer with Samsung Electronics Company Ltd., Suwon, South Korea, since 2015. Her research interests include interference cancellation and signal processing for MIMO systems.
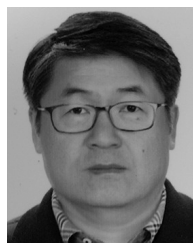
DUCKDONG HWANG (Member, IEEE) received the B.S. and M.S. degrees in electronics engineering from Yonsei University, South Korea, and the Ph.D. degree in electrical engineering from the University of Southern California, in May 2005. He was with Daewoo Electronics, South Korea, as a Research Engineer, from 1993 to 1998. In 2005, he joined the Digital Research Center, Samsung Advanced Institute of Technology, as a Research Staff Member. Since 2012, he has been a Research Associate Professor with the School of Information and Communication Engineering, Sungkyunkwan University, the Electrical Engineering Department, Konkuk University, and the Department of Electronics, Information and Communication Engineering, Sejong University, South Korea. His research interests include physical layer aspect of the next generation wireless communication systems, including multiple antenna techniques, interference alignment and management, cooperative relays and their applications in the heterogeneous small cell networks, and wireless security issues.

CHUNGYONG LEE (Member, IEEE) received the B.S. and M.S. degrees in electronic engineering from Yonsei University, Seoul, South Korea, in 1987 and 1989, respectively, and the Ph.D. degree in electrical and computer engineering from the Georgia Institute of Technology, Atlanta, GA, USA, in 1995. From 1996 to 1997, he was a Senior Engineer with Samsung Electronics Company Ltd., Giheung, South Korea. Since 1997, he has been with the School of Electrical and Electronic Engineering, Yonsei University, where he is currently a Professor. His research interests include array signal processing and communication signal processing.

● ● ●